Spectral Image Prediction of Color Halftone Prints Based on Neugebauer Modified Spectral Reflection Image Model

Masayuki Ukishima 1)4), Yoshinori Suzuki 1), Norimichi Tsumura 1), Toshiya Nakaguchi 1), Martti Mäkinen 2), Shinichi Inoue 3) and Jussi Parkkinen 4)

1) Graduate School of Advanced Integration Science, Chiba University, CHIBA, JAPAN
2) Department of Physics and Mathematics, University of Eastern Finland, JOENSUU, FINLAND
3) Mitsubishi Paper Mills Limited, TOKYO, JAPAN
4) School of Computing, University of Eastern Finland, JOENSUU, FINLAND

Abstract

As the spectral prediction model for color halftone prints using the microscopic measurement, the conventional spectral reflection image model (SRIM) is extended by introducing the concept of the conventional spectral Neugebauer Model, and a new prediction model, the Neugebauer modified spectral reflection image model (NMSRIM), is proposed. Compared to the SRIM, the NMSRIM abstracts the spatio–spectral transmittance distribution of ink layer using the limited number of base color functions and the spatial position function for each base color function in order to efficiently predict the reflectance of color halftone prints from a small number of measurements. The NMSRIM separately analyzes the mechanical dot gain and the optical dot gain. The NMSRIM can predict not only the spectral reflectance but also the microscopic spatial distribution of reflectance. The spatial distribution of reflectance is related to the appearance of halftone prints. The methods to obtain the parameters of NMSRIM are also proposed. Several parameters are obtained by measurements and the others are obtained by computational estimations. To evaluate the validity of the NMSRIM, the spatio–spectral distribution of reflectance printed with two inks, cyan and magenta (testing data) is predicted from the measurements of the halftone prints printed with one ink, the unprinted paper, and the solid prints of inks which are the cyan, magenta and blue (training data), where the blue corresponds to the combination of cyan and magenta inks. The spectral prediction accuracy was significant since the average and maximum values of ΔE_{94} in all samples were 0.66 and 1.30, respectively. We also obtained the interesting results according to the spatial prediction accuracy.

Introduction

In recent years, the image information is changed to digital form with dizzying speed. The digital image is captured, recorded, transferred, analyzed, printed and output with various imaging devices such as digital still cameras, scanners, various types of printers and various types of displays. To share the color information of image between imaging devices efficiently, the color management system (CMS) is important. The concept of CMS is that the color information of image is managed in the form of not a device dependent color but a device independent color such as the CIE XYZ value, the CIE L*a*b* value and the spectral reflectance. The spectral reflectance is the most versatile value since it is not influenced by the illumination environment. The CIE XYZ (or L*a*b*) value on the arbitrary illumination environment can be calculated from the spectral reflectance.

To incorporate an imaging system to CMS, the color reproduction of the system need to be comprehended. From its linearity of the additive color mixture, it is not a hard work to predict the color reproduction of cameras, scanners and displays from a small number of measurements. However, compared to systems based on the additive color mixture, it is difficult to predict the color reproduction of the "printing" system based on the subtractive color mixture due to its nonlinearity. The printing system prints the image as a halftone image where it is constituted as an on–off image of ink dots microscopically. Since the input light into the halftone print is mainly attenuated by the ink region, the reflectance is related to the coverage of ink. However, since the light scattering in paper causes the optical dot gain, the nonlinear relationship is occurred between the reflectance and ink coverage.

A lot of color patches are printed and their color characteristics are obtained by the reflectance measurement. The most primitive solution to comprehend its reproduction is to measure the all combinations of inputs to printer. However, it is not a practical method since too many color patches need to be measured. The second solution is the interpolation–based method using a look up table (LUT). The LUT is generated from not measurements of all combinations but several measurements. The unknown color values are mathematically interpolated and estimated using LUT. However, due to the nonlinearity of printing system mentioned above, one still needs a lot of measurements for high estimation accuracy. The third solution is the prediction–based method using prediction models. This is the most efficient solution since the nonlinearity can be described in the prediction models. Using the limited measurement values, the unknown color values are predicted by the prediction model. The problems are how the prediction model is defined and how the parameters included in the model are obtained.

The reflectance measurement can be done by the macroscopic measurement or the microscopic measurement. The macroscopic measurement is generally based on the point measurement with the spectrophotometer, the spectroradiometer and the macro–densitometer. On the other hand, The microscopic measurement is based on the image measurement with the reflection optical microscope and the micro–densitometer.

In the current printing industry, the macroscopic measurement is generally used because of its advantages where the measurement time and data size are smaller than that of microscopic measurement. Additionally, a lot of prediction models for data obtained by the macroscopic measurement have been proposed such as Murray–Davies equation [1], Yule–Nielsen equation [2], Neugebauer equation [3], Yule–Nielsen modified Neugebauer equation [4], Clapper–Yule model [5], extended Clapper–Yule

model [6, 7], Williams–Clapper model [8], extended Williams–Clapper model [9], generalized model of Clapper–Yule and Williams–Clapper models [10], reflectance and transmittance model for recto-verso halftone prints [11, 12, 13], Kubelka–Munk model [14, 15], revised Kubelka–Munk model [16, 17, 18], models considering the ink penetration into paper [19, 20, 21], and a model considering the fluorescent effect [22].

On the other hand, the microscopic measurement has several disadvantages where it is time–consuming for measurement, the measured data size is large since the data is the (spectral) image, few prediction models have been proposed to analyze the data obtained by the microscopic measurement, and the parameters of the models are difficult to obtain compared to the case of the macroscopic measurement. However we use the microscopic measurement in this research because of the following advantages.

- Accurate dot gain analysis can be done since the dot gain effect can clearly be observed in halftone micro–structure.
- The measured data can be applied to analyze not only color reproduction but also granularity and sharpness since the measured data is the microscopic image (spatial or spatio–spectral reflectance distribution).
- The detail analysis can be done for paper and ink themselves. The results would directly be applied to the development of paper and ink.

In this research, we propose a new prediction model based on the microscopic measurement in order to efficiently predict the spatio–spectral reflectance distribution of color halftone prints from a small number of measurements. The validity of the proposed model is evaluated and discussed through a prediction experiment.

Conventional Spectral Prediction Models

Spectral Neugebauer Model

The Neugebauer model [3] predicts the CIE XYZ tristimulus values of a color halftone patch as the sum of the tristimulus values of their individual colorants weighted by their fractional dot coverages a_i. By considering instead of the tristimulus values of colorants their respective reflection spectra $r_i(\lambda)$, one obtains the spectral Neugebauer equation [23] given by

$$r(\lambda) = \sum_i a_i r_i(\lambda), \tag{1}$$

where $r(\lambda)$ is the spectral reflectance of color halftone patch and the suffix i indicates the color of ink. In color prints using three inks, cyan, magenta and yellow, for example, i indicates cyan c, magenta m, yellow y (primary colors), red r, green g, blue b (secondary colors), black k (tertiary color) or white p (paper). The spectra $r_i(\lambda)$ corresponds to the solid prints spectra using the ink i. Equation (1) is a simple linear equation with the parameters a_i. However, Eq. (1) cannot precisely predict the spectra of color halftone prints due to the dot gain effect. Dot gain is phenomena in printing whereby the printed image becomes to be darker than intended. The dot gain effect can be classified to two types: One is a mechanical dot gain and the other is an optical dot gain. Due to the viscosity of ink, the shape of printed ink dot is changed compared to the intended shape. This phenomenon is called as the mechanical dot gain or the physical dot gain. Due to the mechanical dot gain, the printed dots are generally printed bigger than intended, In other words, the dot coverage of actually printed is bigger than that of intended, where the intended dot coverage is called as *a nominal dot coverage* and the actually printed dot coverage is called as *a effective dot coverage*. On the other hand, the optical dot gain called also as the Yule–Nielsen effect is caused by the light scattering in paper. Due to the light scattering in paper, the printed dots are perceived bigger than actually printed. Additionally, the perceived ink dot is blurred. Therefore, the optical dot gain affects not only color reproduction of the print but also granularity and sharpness of the print. Even if the dot coverages a_i denote the effective dot coverage, the prediction accuracy of Eq. (1) still poor due to the optical dot gain.

Yule–Nielsen Modified Spectral Neugebauer Model

Yule and Nielsen proposed their model to correct the prediction error caused by the dot gain for the black and white prints [2]. Viggiano applied the Yule-Nielsen model to the Neugebauer equation [4] . The Yule-Nielsen modified spectral Neugebauer equation is given by

$$r(\lambda) = \left\{ \sum_i a_i r_i(\lambda)^{1/n} \right\}^n. \tag{2}$$

Equation (2) is a nonlinear equation which corrects the prediction error caused by the dot gain by a parameter n. However, the parameter n is just an empirical value and has no physical meaning. If one changes the printing conditions such as the usage of different paper, different ink and different resolution of print, the parameter n has to be re–estimated from a lot of measurement of spectra.

Spectral Reflection Image Model

Ruckdeschel and Hauser [24] and Inoue *et al.* [25] have proposed the same kind of prediction model having parameters which can provide the physical meaning of the dot gain effect given by

$$r(x,y) = \mathfrak{F}^{-1}\left[\mathfrak{F}\{t(x,y)\}\,\mathrm{MTF}_p(u,v)\right] r_p t(x,y). \tag{3}$$

where (x,y) denotes the spatial coordinates, (u,v) denotes the spatial frequency coordinates, $r(x,y)$ is the spatial distribution of reflectance from the halftone print, $t(x,y)$ is the transmittance spatial distribution of ink layer, $\mathrm{MTF}_p(u,v)$ is the modulation transfer function (MTF) of paper, r_p is the reflectance of paper, and $\mathfrak{F}$ and $\mathfrak{F}^{-1}$ denote the operation of Fourier transform and inverse Fourier transform, respectively. Inoue *et al.* named this equation as a reflection image model (RIM). Figure 1 illustrates the light transfer behavior of RIM. The RIM expresses the halftone print as a spatial distribution of reflectance where the ink dots are superposed on paper, and it is assumed that the ink layer and paper can be optically separated. The light transfer behavior of RIM can be explained as the following steps.

1. The halftone print is illuminated by the input light.
2. The light is partly absorbed and transmitted in the ink layer by its transmittance $t(x,y)$.
3. The transmitted light enters into the paper.
4. The light is scattered in paper by $\mathrm{MTF}_p(u,v)$ and reflected by the reflectance r_p.
5. The reflected light is partly absorbed and transmitted in the ink layer by $t(x,y)$ again before output.

In the RIM, the function $r(x,y)$ is affected by the mechanical dot gain and the optical dot gain, where the mechanical dot gain effect is expressed in the function $t(x,y)$, and the optical dot gain effect is expressed in the function $\mathrm{MTF}_p(u,v)$.

The RIM can directly be extended to a spectral form. The spectral reflection image model (SRIM) is given by

$$r(x,y;\lambda) = \mathfrak{F}^{-1}\left[\mathfrak{F}\{t(x,y;\lambda)\}\,\mathrm{MTF}_p(u,v)\right] r_p(\lambda) t(x,y;\lambda). \quad (4)$$

where λ denotes wavelength, $r(x,y;\lambda)$ is the spatio–spectral reflectance distribution of the color halftone print, $t(x,y;\lambda)$ is the spatio–spectral transmittance distribution of the ink layer and $r_p(\lambda)$ is the spectral reflectance of paper. To be exact, the function $\mathrm{MTF}_p(u,v)$ should also be a spectral form i.e. $\mathrm{MTF}_p(u,v;\lambda)$. We, however, assumed the paper's MTF is independent on wavelength since the wavelength dependence of paper's MTF is not significant [26].

The functions $r(x,y;\lambda)$ and $r_p(\lambda)$ in the SRIM can be measured with a reflection optical microscope attached with a liquid crystal tunable filter (LCTF). A problem of the SRIM (RIM) was difficulty to obtain the functions $\mathrm{MTF}_p(u,v)$ and $t(x,y;\lambda)$. With respect to $\mathrm{MTF}_p(u,v)$, we have proposed a method to efficiently and accurately measure the $\mathrm{MTF}_p(u,v)$ with the reflection optical microscope [26], where $\mathrm{MTF}_p(u,v)$ is calculated by the fraction between two images of the pencil light response in Fourier domain where the two images are reflection images from the paper and the perfect specular reflector. From our measurement results, we concluded that $\mathrm{MTF}_p(u,v)$ of various types of paper can be approximated by

$$\mathrm{MTF}_p(u,v) \approx \frac{1}{\sqrt{1+(2\pi d)^2(u^2+v^2)}}, \quad (5)$$

where d is a fitting parameter which has different value in different paper. On the other hand, with respect to $t(x,y;\lambda)$, we have proposed a method to estimate the function using a computational iteration algorithm [27] as a following procedure.

1. The iteration is performed to each wavelength λ, respectively.
2. Arbitrary spatial distribution is set to $t(x,y;\lambda)$ (Initialization).
3. One substitutes $t(x,y;\lambda)$ to Eq. (4) and obtained a predicted $\hat{r}(x,y;\lambda)$.
4. A signed prediction error function $e(x,y;\lambda)$ is calculated by

$$e(x,y;\lambda) = r(x,y;\lambda) - \hat{r}(x,y;\lambda). \quad (6)$$

5. A root mean square error (RMSE) of $e(x,y;\lambda)$ is calculated by

$$e(\lambda) = \sqrt{\frac{1}{l_x l_y}\int_0^{l_y}\int_0^{l_x}\{e(x,y;\lambda)\}^2 dxdy}. \quad (7)$$

   where l_x and l_y are the horizontal and vertical lengths of image $e(x,y;\lambda)$, respectively.
6. If the RMSE $e(\lambda)$ is sufficiently small value, the iteration is stopped. The current $t(x,y;\lambda)$ is the estimation result. Otherwise, one goes to the next step.
7. One sets $t(x,y;\lambda) + e(x,y;\lambda)$ as a new $t(x,y;\lambda)$.
8. Return to process 3.

Proposed Model: Neugebauer Modified Spectral Reflection Image Model

The spectral Neugebauer model described in Eq. (1) simply expresses the spectral reflectance of the halftone print as the limited number of base functions $t_i(\lambda)$ and their weights a_i. The number of i is only eight when three primary inks are used; cyan, magenta and yellow. In this section, the concept of the Neugebauer Model is applied to the SRIM to increase the efficiency of prediction. As an extended version of the SRIM, we propose a new spectral prediction model named as a Neugebauer modified spectral reflection image model (NMSRIM).

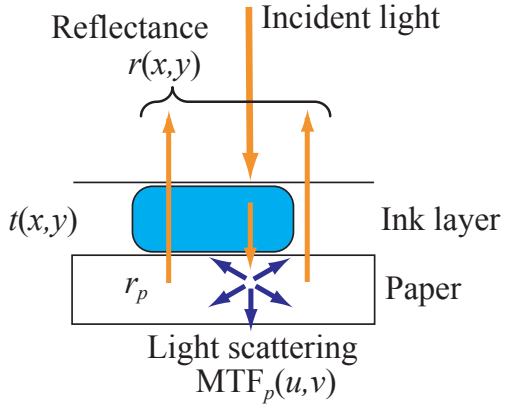

Figure 1. *Light transfer behavior in RIM.*

Transmittance–based Neugebauer Model

As mentioned above, Eq. (1) practically does not precisely work due to the optical dot gain effect. We also mentioned that the transmittance spatio–spectral distribution of ink layer $t(x,y;\lambda)$ in the SRIM is not affected by the optical dot gain. It implies that the Neugebauer Model practically works in the domain of transmittance of ink layer. Then, we have proposed the transmittance–based spectral Neugebauer Model [27] given by

$$\bar{t}(\lambda) = \sum_i a_i \bar{t}_i(\lambda) \quad (8)$$

with constraints

$$0 \le a_i \le 1 \quad \text{and} \quad \sum_i a_i = 1, \quad (9)$$

where the suffix i contains c, m, y, r, g, b, k and p when three primary inks are used, $\bar{t}(\lambda)$ is the spatial average value of $t(x,y;\lambda)$ and $\bar{t}_i(\lambda)$ is the spatial average value of $t(x,y;\lambda)$ for the solid prints of each color i. Note that when i denotes p, $\bar{t}_i(\lambda)$ indicates the transmittance of ink layer **without** ink, therefore

$$\bar{t}_p(\lambda) = 1. \quad (10)$$

Neugebauer Modified Spectral Reflection Image Model

According to the concept of Eq. (8), we approximate the spatio–spectral transmittance distribution of ink layer $t(x,y;\lambda)$ by an equation given by

$$t(x,y;\lambda) = \sum_i A_i(x,y)\bar{t}_i(\lambda), \quad (11)$$

where

$$A_i(x,y) = \begin{cases} 1 & \text{where ink of color } i \text{ exists} \\ 0 & \text{otherwise} \end{cases} \quad (12)$$

with constraints

$$\frac{1}{l_x l_y}\int_0^{l_y}\int_0^{l_x} A_i(x,y)dxdy = a_i \quad (13)$$

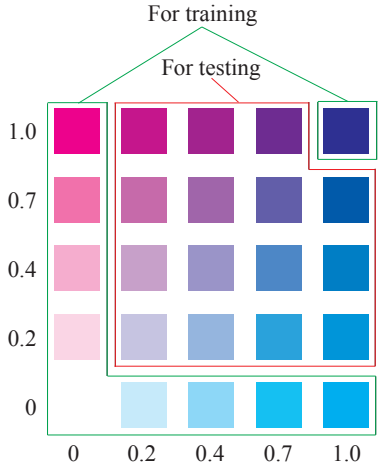

Figure 2. Training data and testing data for the prediction experiment of spatio–spectral distribution of reflectance.

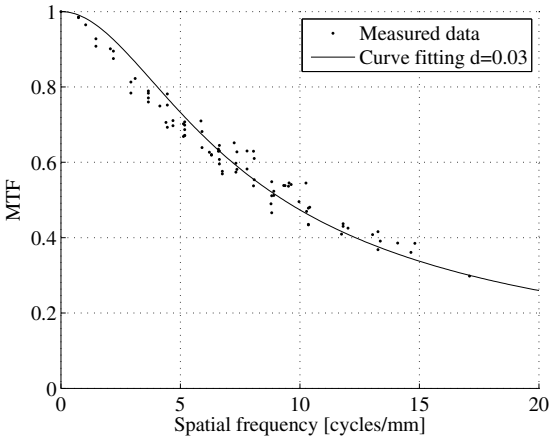

Figure 4. Measured data and fitted curve by Eq. (5) of paper's MTF.

and

$$\sum_i A_i(x,y) = 1 \qquad \text{at all positions in } (x,y). \tag{14}$$

The function $A_i(x,y)$ denotes the positions where the ink of color i which spectrum is $\bar{t}_i(\lambda)$ exists. Equation 11 abstracts the spatio–spectral transmittance distribution of ink layer, $t(x,y;\lambda)$, using the limited number of base color functions $\bar{t}_i(\lambda)$ and the spatial position function $A_i(x,y)$ for each base color function. From Eqs. (4) and (11) the proposed NMSRIM is obtained and given by

$$r(x,y;\lambda) = \mathfrak{F}^{-1}\left[\mathfrak{F}\{\textstyle\sum_i A_i(x,y)\bar{t}_i(\lambda)\}\,\mathrm{MTF}_p(u,v)\right] \cdot r_p(\lambda)\{\textstyle\sum_i A_i(x,y)\bar{t}_i(\lambda)\} \tag{15}$$

Spectral Reflectance Prediction using NMSRIM

In this section, an application of the proposed NMSRIM is discussed through the experiment of spatio–spectral reflectance prediction for a color halftone print. The experimental results are discussed to evaluate the validity of NMSRIM.

Establishment of Research Problem

The research problem is as follows. With respect to the halftone prints printed with cyan and magenta inks, how the spatio–spectral distribution of reflectance printed with two inks (testing data) is predicted from the measurements of limited training data where the training data contain the halftone prints printed with one ink, the un-printed paper, and the solid prints of inks which are the cyan, magenta and blue (Fig. 2), where the blue corresponds to the combination of cyan and magenta inks.

Experimental Conditions

As measurement samples, We used color patches with cyan and magenta inks printed with an offset printer on a coated paper (ISO12642, JAPAN COLOR 2007). The sample patches are composed of twenty five sets of cyan–magenta combination where each nominal dot coverage of cyan or magenta is 0, 0.20, 0.40, 0.70 or 1.00, respectively. The spatio–spectral images of sample patches were measured with a reflection optical microscope (BX50, OLYMPUS) attached with a LCTF (VariSpec CIS Corp., CRI) and with a monochrome CCD camera (INFINITY4–11M, Lumenera Corp., 12–bit quantization, USB 2.0). The images were captured with a spatial resolution of 1024×1024. An

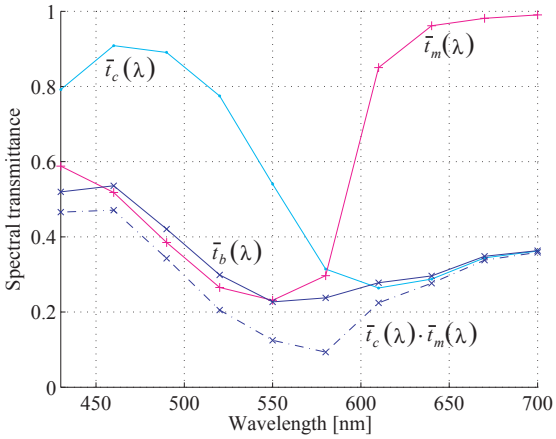

Figure 5. Estimated spectal transmittance $\bar{t}_i(\lambda)$ of cyan, magenta and blue.

objective lens whose magnification power is $4\times$ was used and, in this condition, the vertical and horizontal pixel pitches are 1.96 μm. The spectral resolution of the measurement was set to 30nm in the interval of wavelength 430–700nm [10 bands]. To remove the specular reflection component, two polarizers were attached in front of the camera and the light source, respectively. Divided by a spatio–spectral image of white reference, the measured images were converted to spatio–spectral reflectance factor distributions $r(x,y;\lambda)$.

Experimental Procedure for training

Figure 3 illustrates the schematic diagram for training. The model parameters of the NMSRIM are measured or estimated by a following procedure.

Spectral reflectance of paper $r_p(\lambda)$

From the measurement of un–printed paper, the spectral reflectance $r_p(\lambda)$ is obtained. The function $r_p(\lambda)$ is calculated from the spatial average of the measured image.

MTF of paper $\mathrm{MTF}_p(u,v)$

The MTF of the paper is measured by the our method [26]. We estimate the parameter d in Eq. (5) by a nonlinear optimization. We used a MATLAB function *fminsearch* as the nonlinear optimization tool. In the case of the sample coated paper, d was 0.030. The approximated one dimen-

sional MTF curve of the coated paper is shown in Fig. 4

Spectral transmittance of solid ink layer $\bar{t}_i(\lambda)$

From the measurement of three solid patches with cyan, magenta and blue, the spatio–spectral reflectance distribution $r_i(x,y;\lambda)$ is obtained ($i=\{c,m,b\}$). Using $r_i(x,y;\lambda)$, $r_p(\lambda)$ and $\mathrm{MTF}_p(u,v)$, the spatio–spectral transmittance distribution $t_i(x,y;\lambda)$ is estimated by our computational iteration algorithm. From the spatial average of $t_i(x,y;\lambda)$, the spectral transmittance $\bar{t}_i(\lambda)$ is obtained. Figure 5 shows the estimated spectra $\bar{t}_i(\lambda)$ of cyan, magenta and blue.

Note that we obtain $\bar{t}_b(\lambda)$ not by multiplication of $\bar{t}_c(\lambda)$ and $\bar{t}_m(\lambda)$ but by the measurement of the patch printed with 100% of cyan and magenta inks. In Fig. 5, one can clearly observe that

$$\bar{t}_b(\lambda) \neq \bar{t}_c(\lambda) \times \bar{t}_m(\lambda). \tag{16}$$

Equation (16) is caused by several reasons. One is due to that the SRIM (or RIM) does not consider the light scattering effect in ink layer. If the cyan ink is printed firstly, and the magenta ink is printed secondly on the cyan ink, the larger amount of light input from the upper side of print travels in the magenta ink than in the cyan ink since the several amount of light is scattered and reflected in the magenta ink and it travels only in the magenta ink. This fact derives Eq. (16). The other is due to the lack of trapping which is a phenomenon in the offset printing where in this case the amount of magenta ink printed on the cyan ink dons not correspond to that printed on the paper. The lack of trapping also derives Eq. (16). From Eq. (16), in this research, we obtain $\bar{t}_b(\lambda)$ by the measurement. In other words, we consider that the superposition of two solid inks yields a new colorant, e.g., the superposition of cyan and magenta inks yields the blue colorant.

Spatial position of dots $A_i(x,y)$

The spatial position of dots $A_i(x,y)$ of the halftone patches printed with one ink (cyan or magenta) is estimated. In the case of the print with one ink, Eq. (11) can be rewritten by

$$t(x,y;\lambda) = A_i(x,y)\bar{t}_i(\lambda) + \{1-A_i(x,y)\}\bar{t}_p(\lambda). \tag{17}$$

As we described in Eq. (10), $\bar{t}_p(\lambda)$ is one at all λ, therefore,

$$t(x,y;\lambda) = A_i(x,y)\bar{t}_i(\lambda) + 1 - A_i(x,y), \tag{18}$$

where the formula $1-A_i(x,y)$ corresponds to the spatial positions of un–printed region:

$$1-A_i(x,y) = A_p(x,y). \tag{19}$$

Using Eq. (18), the spatial position of dots $A_i(x,y)$ is estimated by a following algorithm.

1. From the measurement of the halftone patches printed with one ink (cyan or magenta), the spatio–spectral reflectance distribution $r(x,y;\lambda)$ is obtained. Using $r(x,y;\lambda)$, $r_p(\lambda)$ and $\mathrm{MTF}_p(u,v)$, the spatio–spectral transmittance distribution $t(x,y;\lambda)$ is estimated by our computational iteration algorithm. From the spatial average of $t(x,y;\lambda)$, the spectral transmittance $\bar{t}(\lambda)$ is obtained.
2. According to the transmittance–based Neugebauer model described in Eqs. (8) and (9), the effective dot coverage a_i of each halftone patch is estimated by a constrained least square method using $\bar{t}(\lambda)$ and $\bar{t}_i(\lambda)$. We used a MATLAB function *lsqlin* in Optimization Toolbox as a tool of the constrained least square method.
3. A spatial distribution of mean square error $E(x,y)$ is calculated by
$$E(x,y) = \int_\lambda \{t(x,y;\lambda) - \bar{t}_i(\lambda)\}^2 d\lambda. \tag{20}$$
4. Let N is the number of pixels of the error image $E(x,y)$. Then, the number of pixels of ink dot is $a_i N$.
5. For initialization, $A_i(x,y)$ is set to zero at all pixels (x,y).
6. A certain position (x_{min},y_{min}) is searched, where $E(x_{min},y_{min})$ has the smallest value in $E(x,y)$.
7. The pixel $A(x_{min},y_{min})$ is set to one.
8. The pixel $E(x_{min},y_{min})$ is set to ∞.
9. The procedures 6, 7 and 8 are iterated $a_i N$ times.

Experimental Procedure for testing

Figure 6 illustrates the schematic diagram for testing of prediction.

Let $A_i^C(x,y)$ and $A_i^M(x,y)$ are $A_i(x,y)$ of the patches printed with one ink (cyan or magenta), respectively. The functions $A_i^C(x,y)$ and $A_i^M(x,y)$ were estimated in the previous subsection. The first procedure for the prediction of testing patch is estimation of $A_i^{CM}(x,y)$ using $A_i^C(x,y)$ and $A_i^M(x,y)$, where $A_i^{CM}(x,y)$ is $A_i(x,y)$ of the patch printed with two inks (cyan and magenta). The function $A_i^{CM}(x,y)$ for each i is calculated by

$$\begin{array}{lcl} A_c^{CM}(x,y) & = & A_c^C(x,y)\cdot\{1-A_m^M(x,y)\} \\ A_m^{CM}(x,y) & = & \{1-A_c^C(x,y)\}\cdot A_m^M(x,y) \\ A_b^{CM}(x,y) & = & A_c^C(x,y)\cdot A_m^M(x,y) \\ A_p^{CM}(x,y) & = & \{1-A_c^C(x,y)\}\cdot\{1-A_m^M(x,y)\} \end{array}, \tag{21}$$

respectively. Equation (21) is similar to the Demichel's equation.

The second procedure is the prediction of the spatio–spectral reflectance distribution by the NMSRIM described in Eq. (15) using $A_i^{CM}(x,y)$ and parameters measured or estimated from the training data which are $r_p(\lambda)$, $\mathrm{MTF}_p(u,v)$ and $\bar{t}_i(\lambda)$. Therefore, the spatio–spectral reflectance distribution of the patch printed with two inks, $r^{CM}(x,y;\lambda)$, is predicted by

$$\begin{array}{lcl} \hat{r}^{CM}(x,y;\lambda) & = & \mathfrak{F}^{-1}\left[\mathfrak{F}\left\{\sum_i A_i^{CM}(x,y)\bar{t}_i(\lambda)\right\}\mathrm{MTF}_p(u,v)\right] \\ & & \cdot r_p(\lambda)\{\sum_i A_i^{CM}(x,y)\bar{t}_i(\lambda)\} \end{array}. \tag{22}$$

Results and Discussions

As an example of the prediction, a nominal dot coverage combination is shown in Figs. 3 and 6 where that of cyan is 0.4 and that of magenta is 0.2. The predicted spatio–spectral distribution of reflectance, $\hat{r}^{CM}(x,y;\lambda)$, looks similar to the measured $r^{CM}(x,y;\lambda)$. An advantage of the prediction with the NMSRIM that it can predict not only the color but also the spatial appearance. Any other prediction models based on the macroscopic measurement cannot predict the spatial appearance.

Figure 7 compares the measured and predicted results of average spectral reflectance in spatial coordinates with respect to several testing samples:

$$\bar{r}^{CM}(\lambda) = \frac{1}{l_x l_y}\int_0^{l_y}\int_0^{l_x} r^{CM}(x,y;\lambda)\,dxdy. \tag{23}$$

Table 1 shows the ΔE_{94} values between the measured and predicted average spectral reflectance in spatial coordinates with respect to all testing samples. The prediction accuracy was significant since the average ΔE_{94} was 0.66 and the maximum ΔE_{94} was 1.30.

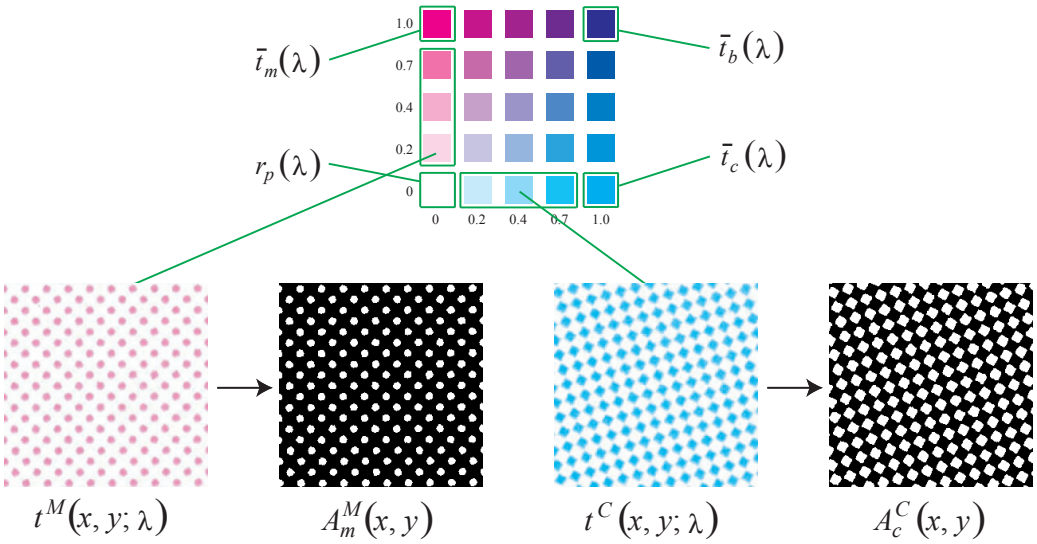

Figure 3. *Schematic diagram for training.*

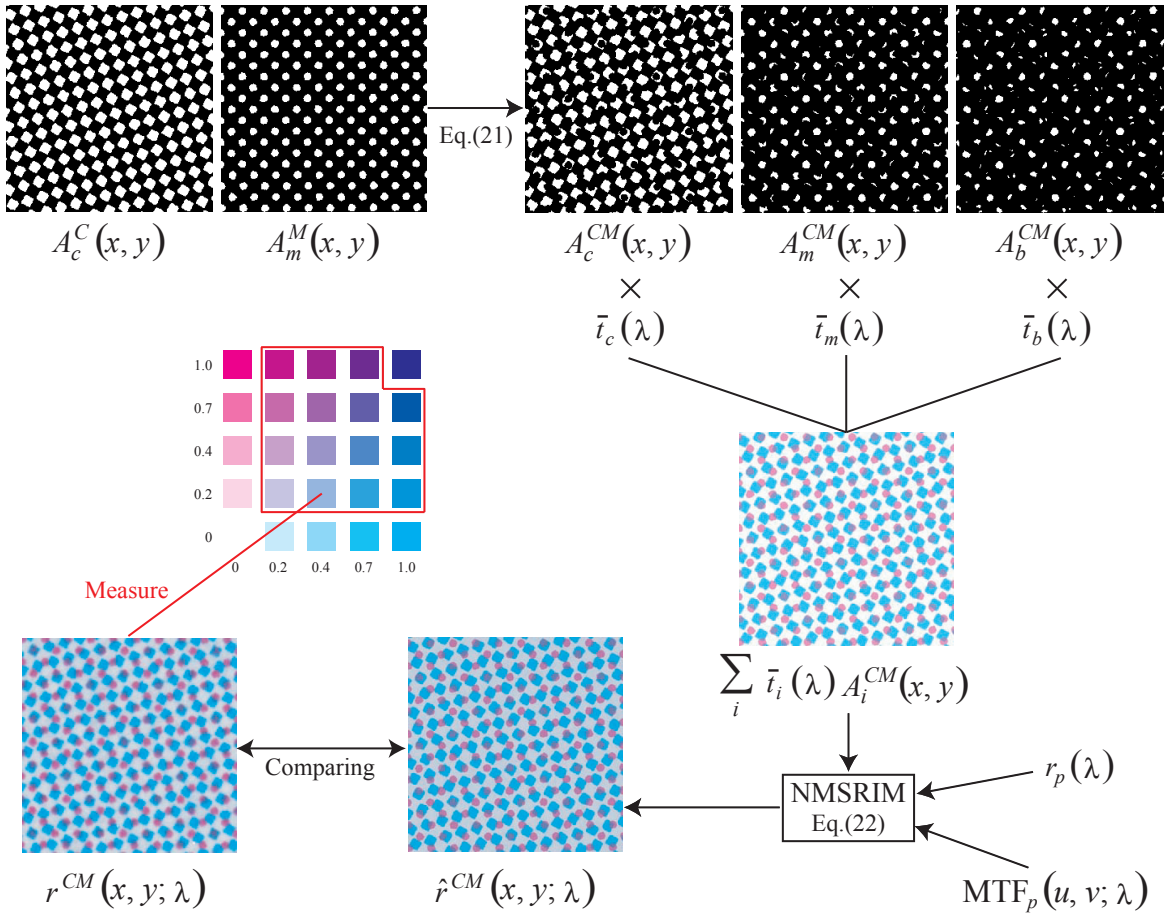

Figure 6. *Schematic diagram for testing.*

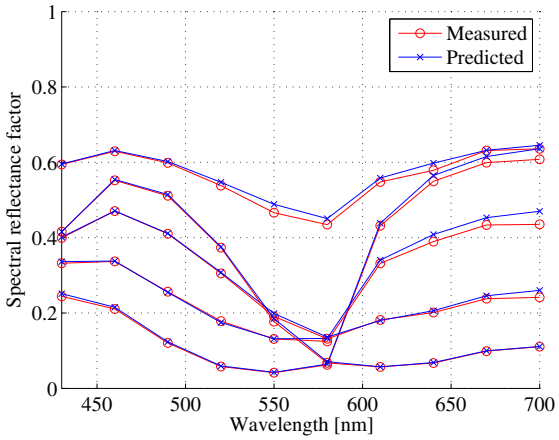

Figure 7. *Measured and predicted results of average spectral reflectance in spatial coordinates with respect to several testing samples.*

Table 1: ΔE_{94} values between the measured and predicted. The average ΔE_{94} was 0.66 and the maximum ΔE_{94} was 1.30.

		Cyan			
		0.2	0.4	0.7	1.0
Magenta	0.2	1.30	0.78	0.82	0.63
	0.4	1.10	0.76	0.62	0.31
	0.7	0.76	0.89	0.46	0.35
	1.0	0.45	0.39	0.31	

Significance of Optical Dot Gain

If one sets $\mathrm{MTF}_p(u,v)$ to one at all spatial frequencies (u,v) in Eq. (22), one can simulate the spatio–spectral distribution of reflectance not affected by the optical dot gain. Figures 8(a) and (b) show the images of simulation results with and without optical dot gain, respectively, where the spatio–spectral reflectance distribution is converted to CIE RGB image on the D65 standard illumination and displayed. Compared to the simulated image with optical dot gain, the simulated image without optical dot gain looks significantly brighter and the dots looks sharper. The optical dot gain significantly affects the appearance of halftone print. Figure 9 shows the difference between average spectral reflectances with and without optical dot gain. It is considered that the NMSRIM significantly corrects the prediction error caused by the optical dot gain.

Conclusion

As the spectral prediction model for color halftone prints based on the microscopic measurement, the conventional spectral reflection image model (SRIM) was extended by introducing the concept of the conventional spectral Neugebauer Model. The proposed new prediction model was named as the Neugebauer modified spectral reflection image model (NMSRIM). Compared to the SRIM, the NMSRIM abstracts the spatio–spectral transmittance distribution of ink layer, $t(x,y;\lambda)$, using the limited number of base color functions $\bar{t}_i(\lambda)$ and the spatial position function $A_i(x,y)$ for each base color function in order to efficiently predict the reflectance of color halftone prints from a small number of measurements. The NMSRIM separately analyzes the mechanical dot gain and the optical dot gain. The NMSRIM can predict not only the spectral reflectance but also the microscopic spatial distribution of reflectance. The spatial distribution of reflectance is related to the appearance of halftone prints. The methods to obtain the parameters of NMSRIM were also proposed. Several parameters were obtained by measurements and the others were obtained by computational estimations. To evaluate the validity of the NMSRIM, the spatio–spectral distribution of reflectance printed with two inks, cyan and magenta (testing data) is predicted from the measurements of the halftone prints printed with one ink, the un-printed paper, and the solid prints of inks which are the cyan, magenta and blue (training data), where the blue corresponds to the combination of cyan and magenta inks. The spectral prediction accuracy was significant since the average and maximum values of ΔE_{94} in all samples were 0.66 and 1.30, respectively. The predicted spatial distribution was visually similar to the measured spatial distribution. The significance of the optical dot gain to the reproduction of color and appearance was also discussed by comparing the simulated results of the spatio–spectral reflectance distributions with and without optical dot gain.

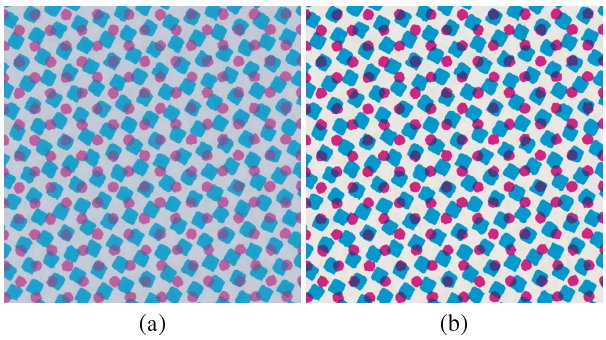

Figure 8. *Images of simulation results with and without optical dot gain. (a) with optical dot gain and (b) without optical dot gain.*

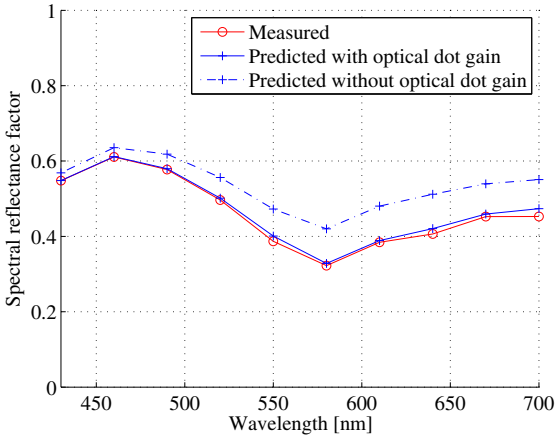

Figure 9. *Difference between average spectral reflectances with and without optical dot gain.*

Acknowledgments

This work was supported by Grant-in-Aid for Specially Promoted Research (19360026).

References

[1] A. Murray, "Monochrome reproduction in photoengraving," J. Franklin Inst. 221, pp.721, 1936.

[2] J. A. C. Yule and W. J. Nielsen, "Penetration of light into paper and its effect on halftone reproduction," TAGA Proc., 65, pp.749–758, 1951.

[3] H. E. J. Neugebauer, "Die theoretischen Grundlagen des Mehrfarbendrucks," Z. Wissen. Photog., 36, pp.36–73, 1937.

[4] J. A. S. Viggiano, "Modeling the color of multi–colored halftones," TAGA Proc., pp.44–62, 1990.

[5] F. Clapper and J. Yule, "The effect of multiple internal reflections on the densities of halftone prints on paper," J. Opt. Soc. Am., 43, pp.600–603, 1953.

[6] P. Emmel and R. D. Hersch, "A unified model for color prediction of halftoned prints," J. Imaging Sci. Technol., 44(4), pp.351, 2000.

[7] G. Rogers, "A generalized Clapper-Yule model of halftone reflectance," Color Res. Appl., 25(6), pp.402, 2000.

[8] F. C. Williams and F. R. Clapper, "Multiple internal reflections in photographic color prints," J. Opt. Soc. Am., 29, pp.595, 1953.

[9] J. D. Shore and J. P. Spoonhower, "Reflection density in photographic color prints: Generalizations of the Williams–Clapper transform," J. Imaging Sci. Technol., 45(5), pp.484, 2001.

[10] M. Hébert and R. D. Hersch, "Classical Print Reflection Models: A Radiometric Approach," J. Imaging Sci. Technol., 48(4), pp.363–374, 2004.

[11] M. Hébert and R. D. Hersch, "Reflectance and transmittance model for recto-verso halftone prints," J. Opt. Soc. Am. A, 23(10), pp.2415–2432, 2006.

[12] M. Hébert, R. D. Hersch and J. M. Becker, "Compositional reflectance and transmittance model for multilayer specimens," J. Opt. Soc. Am. A, 24(9), pp.2628–2644, 2007.

[13] M. Hébert and R. D. Hersch, "Reflectance and transmittance model for recto-verso halftone prints: spectral predictions with multi-ink halftones," J. Opt. Soc. Am. A, 26(2), pp.356–364, 2009.

[14] P. Kubelka, "New Contributions to the Optics of Intensely Light-Scattering Materials. Part I," J. Opt. Soc. Am., 38(5), pp.448–457, 1948.

[15] P. Kubelka, "New Contributions to the Optics of Intensely Light-Scattering Materials. Part II : Nonhomogeneous Layers," J. Opt. Soc. Am., 44(4), pp.330–335, 1954.

[16] L. Yang and B. Kruse, "Revised Kubelka-Munk theory. I. Theory and application," J. Opt. Soc. Am. A, 21(10), pp.1933–1941, 2004.

[17] L. Yang, B. Kruse and S. J. Miklavcic, "Revised Kubelka-Munk theory. II. Unified framework for homogeneous and inhomogeneous optical media," J. Opt. Soc. Am. A, 21(10), pp.1942–1952, 2004.

[18] L. Yang and S. J. Miklavcic, "Revised Kubelka-Munk theory. III. A general theory of light propagation in scattering and absorptive media," J. Opt. Soc. Am. A, 22(9), pp.1866–1873, 2005.

[19] L. Yang and B. Kruse, "Modeling Ink-penetration for Ink-jet Printing," Proc. IS&T's NIP-17: International Conference on Digital Printing Technologies, IS&T, Springfield, VA, pp.731–734, 2001.

[20] L. Yang, B. Kruse and R. Lenz, "Light Scattering and Ink Penetration Effects on Tone Reproduction," J. Opt. Soc. Am. A, 18(2), pp.360–366, 2001.

[21] L. Yang and A. Fogden, "A novel method for studying ink penetration of a print," Nordic Pulp Pap. Res. J., 20, pp.399–405, 2005.

[22] R. D. Hersch, "Spectral prediction model for color prints on paper with fluorescent additives," J. Electronic Imaging, 14(3), pp.33001–12, 2005.

[23] R. D. Hersch, P. Emmel, F. Collaud and F. Crété, "Spectral reflection and dot surface prediction models for color halftone prints" Appl. Opt., 47(36), pp.6710–6722, 2008.

[24] F. R. Ruckdeschel and O. G. Hauser, "Yule-Nielsen effect in printing: a physical analysis," Appl. Opt., 17(21), pp.3376–3383, 1978.

[25] S. Inoue, N. Tsumura and Y. Miyake, "Measuring MTF of Paper by Sinusoidal Test Pattern Projection," J. Imaging Sci. Technol., 41(1), pp.657–661, 1997.

[26] M. Ukishima, H. Kaneko, T. Nakaguchi, N. Tsumura, M. Hautakasari, J. Parkkinen, Y. Miyake, "A Simple Method to Measure MTF of Paper and its Application for Dot Gain Analysis," IEICE Trans. on Fundamentals, Vol.E92-A, No.12, pp.3328-3335, 2009.

[27] M. Ukishima, Y. Suzuki, N. Tsumura, T. Nakaguchi, M. Mäkinen, J. Parkkinen, "A Method to Separately Model Mechanical and Optical Dot Gain Effects in Color Halftone Prints," TAGA Proc., 2010 (in Print).

Author Biography

Masayuki Ukishima *received the B.E. and M.E. degrees from Chiba University, Chiba, JAPAN in 2005 and 2007, respectively. Currently, he is a doctoral course student at the Graduate School of Advanced Integration Science, Chiba University, Chiba, JAPAN. He is also a doctoral course student at the School of Computing, University of Eastern Finland, FINLAND. His current research interests include the image analysis of hardcopy and image quality evaluation and prediction.*

Yoshinori Suzuki *received the B.E. degree from Chiba University, Chiba, Japan in 2009. Currently, he is a master course student at the Graduate School of Advanced Integration Science, Chiba University, Chiba, Japan. His current research interests include the evaluation and prediction of image quality and appearance of hardcopy.*

Norimichi Tsumura *received the B.E., M.E. and Ph.D. degrees in Applied Physics from Osaka University in 1990, 1992 and 1995, respectively. He moved to the, Chiba University in April 1995, as an Assistant Professor. He is currently Associate Professor in Chiba University. He got Charles E. Ives Award (Journal Award: IS&T) in 2002, 2005. He is interested in the color image processing, computer vision & graphics and biomedical optics.*

Toshiya Nakaguchi *received the B.E., M.E., and Ph.D. degrees from Sophia University, Tokyo, Japan in 1998, 2000, and 2003, respectively. From 2006 to 2007, he was a research fellow in Center of Excellence in Visceral Biomechanics and Pain, in Aalborg Denmark from 2006 to 2007. Currently, he is an Assistant Professor at the Graduate School of Advanced Integration Science, Chiba University, Japan. His current research interests include the computer assisted surgery and medical VR training.*

Martti Mäkinen *graduated as a M.Sc. 1998 (University of Joensuu, Finland) and as Ph.D. 2007 (University of Joensuu, Finland). Makinen worked as a research manager at ACA Systems Oy (Polvijärvi, Finland) 1997-99. Since 1999 he has worked (teaching and research) at university of Joensuu, department of physics and mathematics. Current research interests are applied color theory and optical properties of papers and prints.*

Shinichi Inoue *is general manager of process development laboratory, Mitsubishi Paper Mills Limited. He received Ph.D. degree in information science from Chiba University, Japan in 1999.*

Jussi parkkinen *is a professor of Computer Science and the Vice Rector responsible of research at the University of Joensuu, Finland. He specializes in spectral color image analysis, pattern recognition. He received his M.Sc. in medical physics in 1982 and his Ph.D. in mathematics in 1989, from the University of Kuopio, Finland. Since 1999 he has been a professor of Computer Science and since 2007 the vice rector at the University of Joensuu, Finland. Since 2007 a visiting professor at the Chiba University, Japan.*